

INVESTIGATION OF CRITICAL CAPILLARY NUMBER FOR GAS-WATER SYSTEM THROUGH EXPERIMENT AND RESERVOIR SIMULATION

Minghua Ding^{1,2} and Apostolos Kantzas^{1,2}

1: Department of Chemical and Petroleum Engineering, University of Calgary

2: TIPM Laboratory

This paper was prepared for presentation at the International Symposium of the Society of Core Analysis held in Toronto, Canada, 21-25 August, 2005.

ABSTRACT

Residual gas saturation is important in determining recovery from a gas reservoir with water influx. This research addressed residual gas saturation and other variables resulting from spontaneous and forced imbibition tests in porous media.

A new Critical Capillary Number for gas-liquid system was investigated through experimental procedures and numerical reservoir simulations. Capillary pressure curves and relative permeability curves were extracted from the spontaneous experimental data and were further applied to 1D and 3D numerical simulations to simulate the experimental data from co-current and counter-current spontaneous imbibition tests. Relative permeability curves were also calculated from forced co-current imbibition, which followed primary spontaneous imbibition. Different 1D numerical simulation models were then used to simulate the data from forced imbibition experiments. The simulations showed the important role of gas compressibility and verified the residual gas saturation. Under the effect of gas compressibility, the Critical Capillary Number for gas-liquid systems is significantly decreased compared to the conventional number for oil-water systems. Sensitivity studies for different variables were also addressed in the simulation and it was found that the capillary pressure curve is the crucial parameter in the spontaneous imbibition tests but it is no longer important in the forced imbibition tests.

INTRODUCTION

Trapped gas saturation can be very significant in gas reservoirs with water influx. The amount of trapped gas depends on the rate of water influx. After gas gets trapped, increasing capillary number is the key factor to remobilize the residual gas.

Reservoir pressure and residual gas saturation to water drive are two aspects of water influx that would affect recovery. If water influx were strong, the reservoir pressure would remain nearly constant during the life of the reservoir. If water influx were weak, reservoir pressure would continue to decline. The same residual gas saturation as percentage of pore volume in the water-invaded rock would represent a greater amount of trapped gas for the high-pressure case than for the declining pressure case.

Capillary number is defined as the ratio of viscous forces to the capillary forces. Capillary number can be used to describe the relative importance of viscous forces to capillary forces during immiscible displacement. There are several forms of capillary number. The most common version of capillary number is that of Saffman and Taylor (1958):

$$N_{ca} = \frac{v\mu}{\sigma} \quad (1)$$

When the non-wetting phase is trapped in a porous medium, the pressure gradient required to move the non-wetting phase through a capillary tube is much higher than what would be predicted by the pipe flow equation, because of the pressure discontinuity at the wetting/non-wetting interface. Due to the contact angle hysteresis, this discontinuity is not of the same magnitude on the both sides. As an oil drop is pushed through a pore throat, its downstream end gets squeezed into a much narrower segment, making its radius of curvature much smaller than that of the upstream part. Capillary number correlations are only meant for trapping the non-wetting phase. The fraction of non-wetting phase that gets trapped depends on the value of capillary number for the system. Experimental work showed that once the non-wetting phase gets trapped, re-mobilizing it through increasing the displacement velocity is not easy. It generally takes a higher capillary number to re-mobilize the non-wetting phase. Numerous papers have been written on the subject of trapped oil re-mobilization after increasing the capillary number, but much fewer on the subject of re-mobilizing the residual gas saturation. Chatzis and Morrow (1984) performed co-current imbibition tests by building relatively high residual oil saturation from forced imbibition using a small external force gradient, and then gradually increasing the pressure gradient until there was some residual oil production. They found that the critical capillary number for mobilizing the residual oil in porous media is 1×10^{-5} .

Melrose and Brandner (1974) investigated the role of capillary forces in determining microscopic displacement efficiency for oil recovery by water flooding. When non-wetting phase was trapped in porous media, the residual oil ganglia usually extended to no more than about 10 neighboring pores. If the capillary number was increased, which was caused by a higher water flow rate, the isolated oil ganglia were forced to flow. This flow was accompanied by at least two individual displacement events, or rheons. One would be drainage, in which oil moves out of the original volume occupied by the ganglion. The other one would be imbibition, by which water would move into the original volume. The drainage rheon (xeron) occurs at downstream or low-pressure side of ganglion; the imbibition rheon (hygron) occurs at the upstream or high-pressure side. When a critical capillary number is achieved, the residual non-wetting phase saturation will be reduced.

As the displacement of oil by water proceeds, the oil phase eventually disintegrates into blobs of residual oil, which are immobilized by capillary forces. This trapped oil can be removed when the capillary number increases (Larson *et al.*, 1980). They noted that the

disconnections, which occurred as the nonwetting fluid was displaced at a low capillary number, create the residual non-wetting phase fluid. They observed that the high saturation connected fluid is more readily recoverable than the disconnected fluid of saturation remaining after a low capillary number flood. The trapped blobs, which constitute the residual saturation, vary greatly, one from another, in size and shapes, and hence also in capillary number required to mobilize them. The experimental work by Ng *et al.* (1978) confirmed that the capillary number at which a stationary blob becomes unstable and is mobilized or dislodged from its position in the porous matrix is inversely proportional to the length of the blob in the flow direction.

Dong *et al.* (1998) developed a ‘complete’ capillary number by considering the length L and radius R of a capillary tube. The complete capillary number was presented as:

$$CA = \frac{4Ca}{\cos \theta_A} \frac{L}{R} \quad (2)$$

It was further used to characterize saturation profile histories measured in imbibition and in waterfloods. When the ‘complete’ capillary number is much less than 1, capillary forces control imbibition and the saturation rises uniformly along the entire length of the plug. When the ‘complete’ capillary number is much greater than 1, viscous forces control imbibition and there is a step change in saturation from the connate water to the residual oil value, advancing as a piston.

Vizika *et al.* (1994) performed experimental and theoretical studies on the role of viscosity ratio during low-capillary-number forced imbibition in porous media. Through a network model, over a wide range of capillary number, the effect of viscosity ratio on immiscible micro-displacement was investigated. In agreement with the experimental observations, the simulator predicted that the microfingers are formed for any value of viscosity ratio for low capillary numbers; the formation of microfingers is reduced as capillary number increases or viscosity ratio decreases.

Morrow (1979) studied the interplay of capillary, viscous and buoyancy forces in the mobilization of residual oil in porous media. The blobs trapped by capillary forces respond to changes in viscous or buoyancy forces acting on the blob by changes in surface curvature. At ultra-low interfacial tensions, it corresponds to a high capillary number. Capillary number was also investigated at three types of wetting fluids in sphere packs. Although capillary forces are expected to be reduced with an increase in contact angle, the pressure of mobilization was not necessarily reduced, since both the contact-angle hysteresis and the interaction of pore geometry and contact angle were involved in the effect of wettability on resistance to mobilization by capillary forces.

Morrow and Songkran (1981) investigated the effect of viscous and buoyancy forces in the mobilization of non-wetting phase in porous media. The trapping of residual non-wetting phase in the packing of equal spheres had been investigated for a wide range of capillary numbers and Bond numbers. Bond number is defined as the ratio of gravity to

capillary forces. For vertical displacement, the residual saturation varied from normal value of about 14.3% when the Bond number was less than 0.00067 and capillary number was less than 3×10^{-6} , down to near zero when either the bond number exceeded 0.35 or capillary number exceed about 7×10^{-4} . It was estimated that mobilization of trapped blobs is about five times more difficult to achieve than prevention of trapping. When the capillary number and Bond number are well below their critical values, capillary forces dominate the displacement.

Constantinides and Payatakes (1991, 1996) investigated the coalescence of ganglia in porous media through a theoretical model and network simulation. The wetting phase saturation, viscosity ratio, capillary number, and the probability of coalescence between two colliding ganglia were investigated. They observed that the probability of coalescence between pairs of moving ganglia increased weakly as the capillary number increased. The results also indicated an increasing tendency of ganglia to move through the large pores when the capillary number decreased.

EXPERIMENTAL

Preparation of Samples and Liquids

Two Berea sandstone plugs and four sandstone plugs were used in the experiments. The plugs are approximately 3.81 cm (1.5") in diameter and 5.08 cm (2") in length. Before the experiments, the plugs were cleaned in the Dean Stark apparatus and were dried in the oven at about 105°C until the mass of plugs became constant. Porosity and air permeability were measured. The basic parameters for all the plugs used are summarized in Table 1.

Plug ID	l	d	K_{air}	K_{brine}	ϕ
	cm	cm	md	mD	%
SIII-1	5.065	3.84	608.5	71.5	15.89
SIII-3	5.01	3.86	45.57	12.47	5.63
SIII-4	5.07	3.84	378.0	85.74	9.79
SIII-5	5.00	3.86	114.5	25.65	7.09
B-1	5.255	3.805	583.0	400.0	24.01
B-2	5.43	3.805	583.0	400.0	24.01

Table1: Basic properties of the plugs used.

(B-1 and B-2 were sister plugs, permeability and porosity were measured once)

	ρ	μ	σ
	g/cm^3	mPas	mN/m
Oil	0.8112	7.2	25.97
Brine	1.0109	1	72.53

Table 2: Properties of the liquids used

Synthetic reservoir brine was used for the Western Canada sandstone plugs, 2% NaCl brine was used for Berea sandstone plugs. The properties of fluids are summarized at Table 2.

Experimental Procedures

Two Berea sandstone plugs were tested first by carrying out water-oil imbibition. The plugs were saturated with oil to 100% saturation. Then water was allowed to spontaneously imbibe into the plugs until no more oil was produced (S_{or}). At the end of spontaneous imbibition, water was injected, at different flow rates (forced water imbibition). When the flow rate reached a certain value, oil production started again. The oil produced as well as the flow rate, and pressure drop across the plug were recorded. The corresponding capillary number was calculated.

After the water-oil imbibition test was completed, the plugs were cleaned in the Dean Stark apparatus again and were dried in the oven until the weight became constant. Then the same experiments were performed on these two plugs but this time water was the wetting phase and gas (air as the gas phase at this research) was the non-wetting phase. On-line NMR relaxometry was used to monitor the water influx into the core. Forced water imbibition followed the spontaneous imbibition tests. Water saturation changes with time and at different flow rates can then be calculated through converting the NMR amplitude into imbibed water mass. Gas saturation was calculated at different water flow rates, which corresponds to the capillary number for the water-gas system.

Finally, four Western Canada sandstone plugs were used to repeat the same experiments as for the gas-water system. The objective was to test whether the critical capillary number obtained with the gas-water system in Berea sandstone plugs is general or specific.

At the final flow rate of forced water imbibition, the residual gas saturation for both Berea sandstone plugs and sandstone plugs decreased to almost zero. If we assume the mass transfer between gas and liquid is neglected, the posed the question whether all the gas was recovered or trapped gas bubbles got compressed at higher flow rates. Therefore, at the final flow rate of water imbibition for the sandstone plugs, the injection valve was shut off. NMR measurements continued to measure gas saturation changes with time. If the water saturation increase were due to compressed gas, the gas bubbles would expand in the porous medium and expel more water from the plugs. That would in turn increase the residual gas saturation when the external applied pressure was released.

RESERVIOR SIMULATION

Reservoir Simulation models

The experimental results were simulated numerically, using a three-phase reservoir simulator. The objectives of this phase of the investigation were two-fold. First, it was intended to history match the experimental results through the simulation of spontaneous and forced imbibition processes through the 1D simulation model. Along with that, several variables that affect the final residual gas saturation, such as gas compressibility, were investigated, which are difficult to study experimentally. Then a 3D reservoir simulation model was developed to simulate counter-current imbibition experiments.

Measurement of the Capillary Pressure from the Co-current Spontaneous Imbibition Test

In 1960, Handy introduced the method for determining the effective capillary pressure for porous media from imbibition data. Based on different assumptions, the equation for piston-like displacement was derived. In many respects, the rate of imbibition in porous media is analogous to the rate of capillary rise in capillaries. From this analogy, the assumptions in the derivation of piston-like displacement are that water imbibes in a piston-like manner and the pressure gradient in the gas phase ahead of the water front can be neglected.

$$N_w^2 = \left(\frac{2P_c k_w \phi A^2 S_w}{\mu_w} \right) t \quad (3)$$

In the present spontaneous co-current imbibition tests, it was found that the results were closer to piston-like water displacement. The results indicate that water imbibes into both small pores and large pores simultaneously during spontaneous imbibition.

Calculations of the relative permeability from the Co-current imbibition Test

Calculation of Relative Permeability Curves from Spontaneous Imbibition Test

There is no way to measure relative permeability curves from the spontaneous imbibition tests, except for the effective water permeability values that can be measured at the end of spontaneous imbibition tests. The relative permeability curves were then calculated by employing Corey's equations, which assume the two exponents are equal to 2.

$$k_{rw} = \frac{K_{ew}}{K_w} \left(\frac{S_w - S_{wir}}{1 - S_{wir} - S_{gr}} \right)^{n_w} \quad (4)$$

$$k_{rg} = \frac{K_{eg}}{K_g} \left(\frac{S_g - S_{gr}}{1 - S_{wir} - S_{gr}} \right)^{n_g} \quad (5)$$

Calculation of Relative Permeability Curves from Forced Imbibition Test

Relative permeabilities are very important in reservoir simulation for both spontaneous and forced imbibition. Relative permeability curves for forced imbibition can be measured from the forced imbibition test using the unsteady-state method. When the forced imbibition test was processed, at each flow rate, the pressure drop was measured along the plug and the effective brine permeability was calculated from Darcy's law. Then the relative permeability at the end of each flow rate can be calculated as the ratio of the effective brine permeability at the end of each flow rate to the absolute brine permeability. The water saturation at the end of each flow rate can also be monitored from the amplitude change through NMR, so the relative permeability for water is obtained.

RESULTS AND DISCUSSION

Experimental results

Capillary Number

Figure 1 shows the normalized residual oil saturation changes as a function of capillary number for two Berea plugs for water-oil systems. The results indicate that the residual oil saturation became smaller when the capillary number reached 2×10^{-5} , which is consistent with Chatzis and Morrow's (1984) work. Even though the experimental procedure presented here is different from the one in the literature, the same critical capillary number was obtained when the initial residual oil started to be mobilized. This implies that the critical capillary number is independent of the initial experimental procedure. Once oil gets trapped, it always needs a certain applied viscous force to remobilize.

Figure 2 presents imbibition test results for Western Canada sandstone SIII-1 as an example. In this figure, spontaneous imbibition, forced imbibition, and the gas saturation changes with time, as well as after shutting off injection, can be seen. In the spontaneous imbibition tests, the gas saturation changed fast at the beginning and slowed down subsequently. There was no significant gas saturation change at the lower flow rates, but sudden changes occurred when flow rate reached a certain critical point. From Figure 2 we can see that at the end of forced imbibition tests, the residual gas saturation dropped almost to zero for all the plugs. If all the residual gas were produced, shutting off the injection side would not change the final residual gas saturation. The results show that instead the gas saturation increased. This implies that water saturation increase is only partially attributable to gas production, the remainder being gas compression. When the injection side is shut off, the pressure applied to the plug is released and compressed gas bubbles expand inside the porous medium and displace some water.

The gas normalized gas saturation changes with the capillary number for all plugs are plotted in Figure 3. It shows that the gas saturation does not change significantly until the capillary number reaches 2×10^{-8} , which corresponding the flat part of red color curve in Figure 2 at the low flow rate of spontaneous imbibition tests. This indicates that the critical capillary number is much smaller in gas-water systems than in the corresponding water-oil systems. Thus, it is much easier to remobilize trapped gas bubbles than remobilize trapped oil ganglia.

Capillary Pressure and relative permeability

The calculated results of capillary pressure from spontaneous imbibition tests and relative permeability curve from both spontaneous and forced imbibition tests are shown in Figures 4 and 5. It is difficult to characterize gas relative permeability curve for the forced imbibition part, since at the end of spontaneous imbibition test, the residual gas saturation was reached. The relative gas permeability at this point is zero and the gas is immobile. When forced imbibition is performed at different flow rates, the viscous

forces as well as the capillary number increases. When the capillary number reaches a certain value, the residual gas bubbles are re-mobilized. That means the relative gas permeability is no longer absolutely zero for forced imbibition after the capillary number reaches the critical capillary number. The trapped gas bubbles may be produced, or compressed into smaller bubbles, or dispersed into the water stream, or snap off gradually. All these effects indicate that the original trapped gas bubbles from spontaneous imbibition tests start to re-mobilize.

This “apparent” gas relative permeability was calculated from the forced imbibition data using the following procedure. First, it is assumed that the capillary pressure is negligible. Thus the pressure drop for the gas phase along the sample will be the same as the pressure drop for the water phase and it will be linear. Then the gas saturation decreasing at each flow rate can be measured from increasing of water saturation through NMR equipment. Then the gas volume change in the porous medium can be calculated by multiplying the saturation by the pore volume. The gas flow rate can be calculated using the change of gas volume and the imbibition time at this flow rate. Finally, using Darcy’s Law the effective gas permeability at each water injection rate can be calculated and the gas relative permeability can be obtained.

Reservoir Simulation results

Simulation Results of Co-current Imbibition Tests

Figures 6 and 7 are the comparison results of reservoir simulation from co-current imbibition test during spontaneous and forced imbibition tests. The excellent matches of simulation results with the experimental data indicate the simulation model built, capillary pressure curves calculated, and relative permeability used can perfectly simulate the experimental results. Therefore the effect of gas compressibility investigated through this reservoir simulation model is reliable.

Simulation Results of Counter-current Imbibition Tests

Figure 8 is the comparison results of reservoir simulation from counter-current imbibition test during spontaneous imbibition tests. The capillary pressure curves and relative permeability curves used in the simulation were the same as for co-current imbibition experimental tests for each sample. During both co-current and counter-current imbibition tests, the same pair of water and gas was used. The pore structure of the porous medium for a given sample does not change; therefore the capillary pressure, which is operating in co-current and counter-current imbibition, should be exactly the same. The agreement results between the simulation and experiments proved this view.

Effect of Gas Compressibility on Residual Gas Saturation

From Experimental Results

In order to calculate the true residual gas saturation at the final pressure, the final gas saturation after gas saturation build-up is calculated using the ideal gas EOS to calculate

the corresponding gas volume at the last flow rate for the forced imbibition test. The reason for using ideal gas law is that the maximum pressure drop along the plugs is less than 1400 kPa (200 psi). The calculated gas saturation at the last flow rate of forced imbibition was then compared with the values from experiments. The results obtained were similar, as shown in Figure 9.

From Simulation

Three runs were made on each sample. First run was the normal compressibility (compressibility), second run the less changed gas volume factors (a little compressibility) were used and third the constant gas volume factor was used (zero compressible). The simulation results again prove that the critical capillary number in a water-gas system is much smaller than the corresponding water-oil system and the critical capillary number obtained for the gas-water system is true. This number can slightly vary for different gases. Gas compressibility not only reduced the size of trapped gas bubbles, making it easier for them to move, but also significantly reduced the capillary pressure holding the trapped gas bubbles.

Besides the reasons above, gas dissolved in water was considered another big reason of changing residual gas saturation. In this research, we found that the maximum pressure drop applied on sample was 200psi and the air solubility at this pressure is extremely small. So we did not take into account of the effect of dissolved gas on residual gas saturation. In the real gas reservoir, which the pressure drawdown can be as high as 5000psi, the effect of dissolved gas on residual gas saturation will be very pronounced and must be taken into account.

CONCLUSIONS

- The critical capillary number for gas-water system was investigated from both experiment and numerical simulation.
- The critical capillary number to re-mobilize trapped gas in a gas-water system was found to be much smaller (2×10^{-8}) than the corresponding number for an oil-water system (2×10^{-5} from literature), which was also reproduced in this research.
- After the end point capillary pressure was calculated from Handy's model, the full imbibition capillary pressure curves were obtained assuming $P_c \propto 1/S_w$ and were proved correct through reservoir simulation.
- The relative permeability curves were calculated from forced imbibition.
- The effect of gas compressibility on residual gas saturation was investigated experimentally and numerically.

ACKNOWLEDGEMENTS

Financial support from TIPM laboratory, the Canada Research Chair in Energy and Imaging and the sponsoring companies Nexen, Canadian Natural, Devon Canada, Petro-Canada, Shell Canada, Albian Sands, E-T Energy is gratefully appreciated.

NOMENCLATURE

A	cross-section area of sample, cm ²	S_{gr}^*	Residual gas saturation at each step of spontaneous imbibition
CA	Complete Capillary number	S_{or}	Residual oil saturation at end of spontaneous imbibition
d	diameter of sample, cm.	S_{or}^*	Residual oil saturation at each step of spontaneous imbibition
K	Absolute air permeability	S_w	Water saturation behind the water front
k_{rw}	Water relative permeability	S_{wir}	Irreducible water saturation
K_w	Effective water permeability at S_{wf}	t	Imbibition time, minute
K_{ew}	Water effective permeability	n_w	Water phase exponent
K_g	Effective water permeability at S_{wf}	n_g	Gas phase exponent
k_{rg}	Gas relative permeability	μ	Viscosity, mPa.s
K_{eg}	Gas effective permeability	ρ	Density, g/cm ³
l	Length of plug, cm.	σ	Interfacial tension, mN/m
N_{ca}	Capillary number	ϕ	Porosity, fraction
N_w	Volume of water imbibed into the core, cm ³	ν	Pore velocity, cm/s
P_c	Capillary pressure at S_{wf}		
S_g	Gas saturation		
S_{gr}	Residual gas saturation		

REFERENCES

1. Chatzis, I. and Morrow N.R., "Correlation of Capillary Number Relationships for Sandstone", *Pet. Trans. AIME*, (1984) **277**, 555.
2. Constantinides, G. N. and Payatakes, A. C., "A Theoretical Model of Collision and Coalescence of Ganglia in Porous Media", *Journal of Colloid and Interface Science*, (1991) **141**, (2), 486.
3. Constantinides, G. N. and Payatakes, A. C., "Network Simulation of Steady-State Two-Phase Flow in Consolidated Porous Media", *AICHE Journal*, (1996) **42**(2), 369.
4. Ding, M. "Gas Trapping and Mobilization through Water Influx in Natural Gas Reservoirs", *PhD Thesis*, (2005) University of Calgary.
5. Dong, M., Dullien, F. and Zhou, J., "Characterization of Waterflood Saturation Profile Histories by the 'Complete' Capillary number", *Transport in Porous Media*, (1998) **31**, 213.
6. Larson, R. G., Scriven, L. E., and Davis, H. T. "Percolation Theory of Two Phase Flow in Porous Media", *Chemical Engineering Science*, (1980) **36**, 57.
7. Melrose, J. C. and Brandner, C.F., "Role of Capillary Force in Determining Microscopic Displacement Efficiency for Oil Recovery by water flooding", *J. Can. Pet. Tech.*, (1974) **13**, 54.
8. Morrow, N. R., "Interplay of Capillary, Viscous and Buoyancy Forces in the Mobilization of Residual Oil", *The Journal of Canadian Petroleum Technology*, (1979), 35.
9. Morrow, N. R. and Songkran, B., "Effect of Viscous and Buoyancy Forces on Nonwetting Phase trapping in Porous Media, in Surface Phenomena in Enhanced Oil Recovery", *D.O. Shah, Editor, Plenum Press*, (1981) 387.
10. Ng, K. M., Davis, H. T. and Scriven, L. E., "Visualization of Blob Mechanics in Flow Through Porous Media", *Chem. Eng. Sci.*, (1978) **33**, 1009.
11. Saffman, P. G. and Taylor, G., "The Penetration of a Fluid into a Porous Medium or Hele-Shaw Cell Containing a More Viscous Fluid", *Proc. Royal Soc. London, Ser.* (1958) **245**, 312.

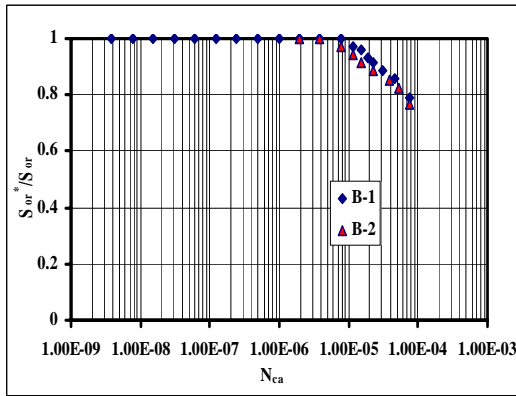


Figure 1: Normalized oil saturation vs. capillary number in oil-water system for Berea sandstone samples B-1 and B-2.

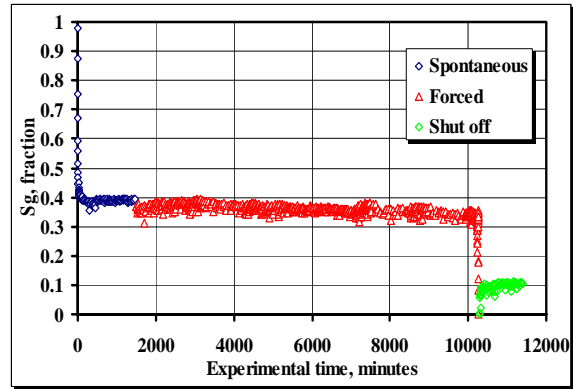


Figure 2: Gas saturation change with time in water-gas system for plug SIII-1.

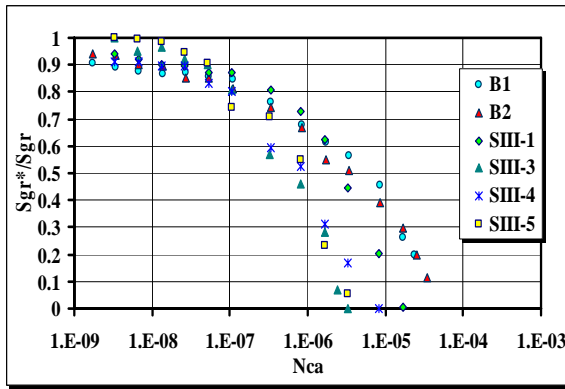


Figure 3: Normalized gas saturation vs. capillary number in gas-water system.

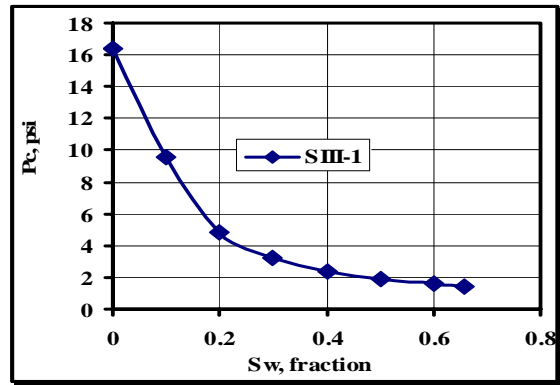


Figure 4: Results of capillary pressure from Handy's model for SIII-1.

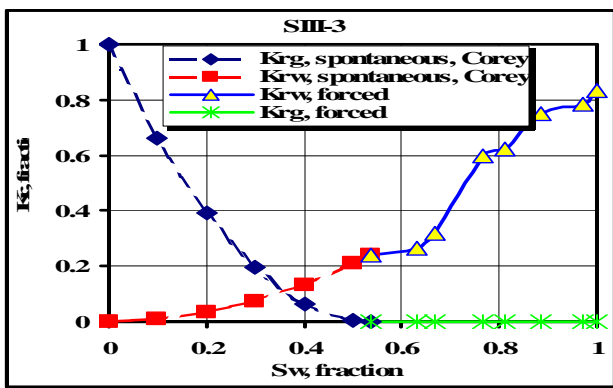


Figure 5: Relative permeability data for plug SIII-1 during spontaneous and subsequent forced imbibition.

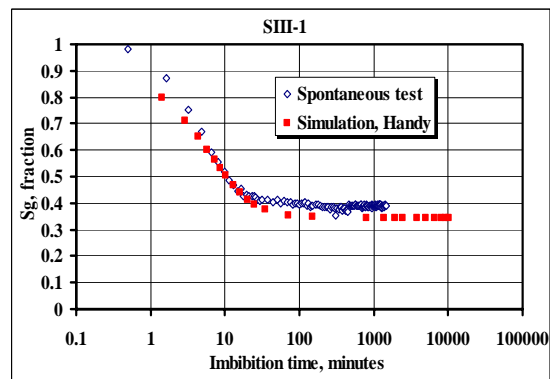


Figure 6: Comparison of 1D simulation with imbibition test for Sample SIII-1.

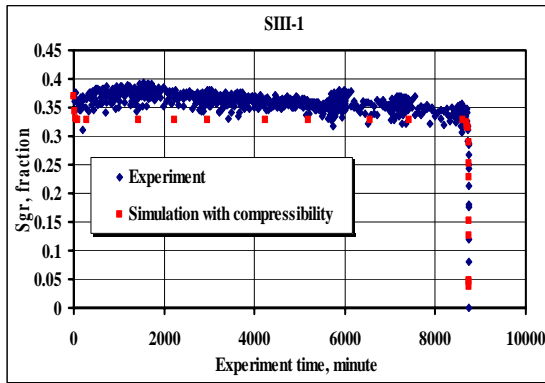


Figure 7: Comparison of results of numerical simulation for plug SIII-1 with forced imbibition tests.

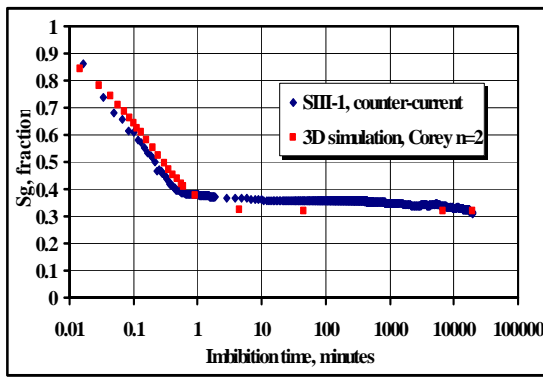


Figure 8: Reservoir simulation results for plug SIII-1 with experimental data for the counter-current spontaneous imbibition test.

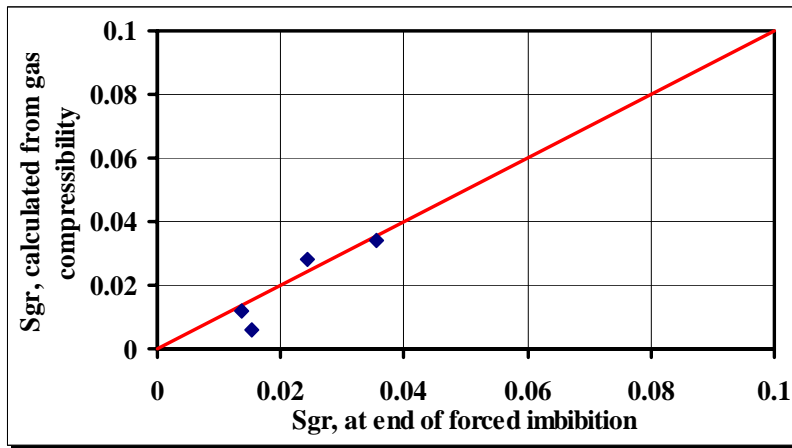


Figure 9: Comparison of results for residual gas saturation from experiments with the values from compressibility calibration.

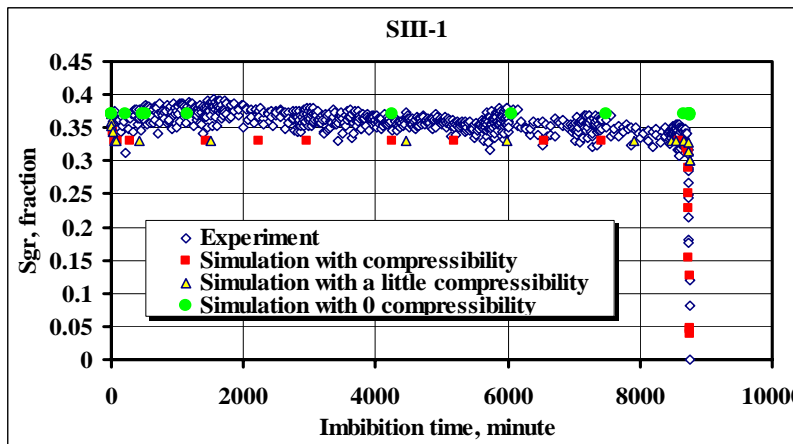


Figure 10: Reservoir simulation results for plug SIII-1 with and without the effect of compressibility and experimental data for the forced imbibition test.